Understanding the Limits of Screening Operation. Part 2: Characterizing the Operational Window

Miguel E. Villalba,[a,*] James A. Olson,[b] and D. Mark Martinez [a]

The limits of the pulp screening operation can be defined as the maximum throughput before the apertures start to plug permanently. This two-part article sought insights into the limits of screening operation. In part two, the operational window of the screen was characterized by performing a series of screening trials with different pulp furnishes, where the plugging point was conventionally measured with the pressure signal. The limits of operation, given by a slot velocity and rotor speed contour, showed a robust linear relationship at the point of plugging, which depended on the ratio of the fibre length to aperture size. For size ratios less than 1.5, the screen did not plug under the conditions tested. In addition, the plugging detection tool was conceptualized in part one based on the kurtosis of the distribution of fluctuation peaks, and it was employed here. Effectively, deviations from the Gaussian distribution of the pressure fluctuation peaks signal the onset of screen plugging. Thus, the utility of this tool was confirmed for detecting plugs using readily available pressure fluctuation data in pilot-scale screening operations.

DOI: 10.15376/biores.19.2.2990-3000

Keywords: Pressure screen; Plugging; Rotor speed; Intermittency; Detection-tool

Contact information: a: Department of Chemical and Biological Engineering, University of British Columbia, 2360 East Mall, Vancouver, V6T 1Z4, BC, Canada; b: Department of Mechanical Engineering The University of British Columbia, 6250 Applied Science Lane, V6T 1Z4, BC, Canada;
** Corresponding author: miguel.villalba@mech.ubc.ca*

INTRODUCTION

This article is part two of a two-part study investigating the limits of screening operations. Part one focused on characterizing the plugging mechanisms occurring in the limits of operation (Villalba *et al.* 2024). Particularly, it elucidated an increased intermittency as a precursory mechanism to screen failure. Part two presents the results of screening trials in which the operational window of the screen is characterized.

The limits of screening operation represent the maximum capacity at which the screen can run before plugging becomes permanent. Although screens can fail in many ways, this study focused on plugging occurring in the screen apertures. Understanding the limits of screening operation is crucial for screen operators to maximize throughput while reducing power consumption and preventing plugging (Salem 2013). These limits are fundamentally dictated by the interplay between fibre deposition (slot velocity), the pressure pulses created by the rotor (rotor speed), and the rheology of the pulp suspension (Martinez *et al.* 1999; Salem 2013). These studies report a linear relationship between rotor speed and slot velocity.

This investigation expanded on previous screening studies and explored further the limits of screening operation using a pilot-scale pressure screen. It used a series of trials, in which different pulp suspensions and screen geometries were employed. As is typically done in industry as well as in other screening studies (Estevez-Reyes 1995; Salem 2013), plugging was monitored using pressure sensors. Unlike other groups, the pressure fluctuations were examined using the statistical tool that was conceptualized in part one of this study to detect the onset of screen plugging. In part two, presented here, the utility of this tool was assessed by characterizing the transition from the operational to the plugged state using the readily available pressure signal for different pulp suspensions.

EXPERIMENTAL

The screening trials were performed with a Beloit MR8 laboratory pressure screen (Fig. 1) similar to that used by Salem (2013). The MR8 is a 212 mm diameter horizontal screen and is equipped with a variable frequency drive (VFD) to control the rotor speed up to 2000 rpm. Note that this is a horizontal screen, and typically larger vertical configurations are used in practice. An Aikawa Fiber Technologies (AFT) foil rotor (Fig. 1b) was used for all trials, but the screen cylinder was changed between trials to test different aperture widths and geometries. The rotor-cylinder gap was kept the same at 6 mm. The pulp was supplied from a 4000 L main stock tank through a feed port. For trials using water, a smaller 1500 L tank was used instead. The main stock tank is fitted with a variable speed repulper or mixer. As only market chemical pulps were used in this study, disintegration was relatively straightforward and there was little debris.

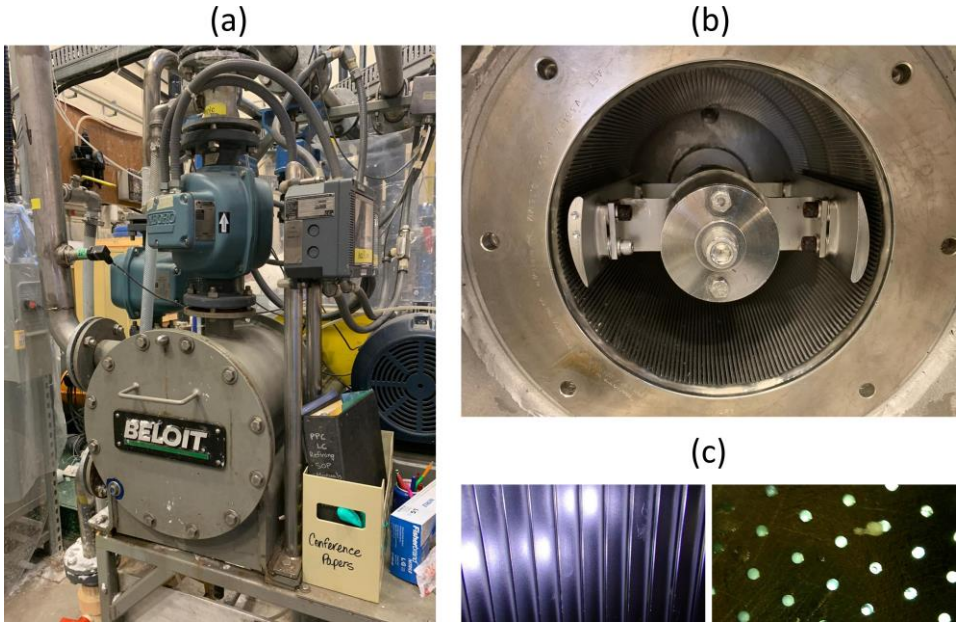

Fig. 1. Beloit MR8 pilot screen shown in panel (a). View of the inside of the pressure screen including the AFT foil rotor and the screen cylinder in panel (b). Panel (c) shows the close-up view of the screen cylinder with two types of apertures used: wedge-wire slots (left) and holes (right)

The reject and accept streams were returned to the feed tank following a loop. Pulp temperature was maintained constant at a nominal value of 30 °C for all trials. The pulp feed consistency was also monitored and kept constant throughout every test. A constant volumetric reject ratio R_v = 0.2 was used for all trials by controlling the accept and reject valves in order to prevent reject thickening. Pulp suspensions of the same mass consistency c = 1.0% were prepared from different sources: Northern Bleached Softwood Kraft (NBSK) pulp from Canfor (Prince George, BC), eucalyptus kraft pulp from Suzano (Brazil), and a specialized short-fibre hardwood-softwood mix pulp from Domtar Inc (Windsor, QC). Note that the latter pulp suspension had been subjected to further treatment to shorten the fibre length significantly. Table 1 summarizes the pulp and screen configurations used for each trial, including the pulp type and the average fibre length ℓ, smallest dimension of the screen aperture width w, and their corresponding size ratio ℓ/w. Screen cylinders with wedge-wire slotted apertures were used for all trials except for trials 7 and 8, which used cylinders with conically-drilled holes. These commonly used screen geometries, supplied by AFT Inc., are depicted in Fig. 1c. Screen A has a slot width of 0.15 mm, a contour height of 1.2 mm, and wire width of 3.2 mm. Screen B has a slot width of 0.1 mm, a contour height of 0.9 mm, and wire width of 3.2 mm. Screen C has a slot width of 0.2 mm, a contour height of 0.9 mm, and wire width of 3.2 mm.. Note that the difference in contour height likely has an effect on plugging. However, this study focused on the effect of slot width, which is deemed to be dominant.

Table 1. Trial Matrix Highlighting the Combinations of Materials (working fluid), Average Fibre Length ℓ, Screen Type, Smallest Dimension of the Width of the Aperture w, Size Ratio ℓ/w, Range of Feed Flow Rates Q_f, Slot Velocity V_s and Range of Rotor Tip Speeds V_t Used *

Trial	Material	ℓ (mm)	Screen	w (mm)	ℓ/w	Q_f (L/min)	V_s (m/s)	V_t (m/s)
1	NBSK	2.5	A	0.15	16	460 to 1500	1-3.5	0-20
2	Eucalyptus	0.7	B	0.1	7	160 to 1000	0.5-3	0-20
3			C	0.2	3.5	230 to 1340		
4	Short Mix	0.3	B	0.1	3	160 to 980	0.5-3	0-20
5			A	0.15	2	180 to 1300		
6			C	0.2	1.5	220 to 1350		
7			D	0.5	0.6	130 to 850		
8			E	0.8	0.4	246 to 1470		
9	Water	0	A	0.15	0	208 to 1300	0.5-3	0-20

* Trials 7 and 8 used screens with drilled holes.

Pressures and flow rates measurements were taken in the feed, accept, and reject lines at a sampling rate of 1000 samples per second *via* pressure transducers (Wika #8351312) and magnetic flow meters (Foxboro 8300 series), respectively. The data were collected and displayed with a LabView program. The data was further processed and analyzed in MATLAB. The pressure signal components, including the moving average and fluctuations, were computed in the same way as the area data described in Eqs. 1 and 2 in part one of this investigation.

The trial protocol involved turning the rotor to a rotational speed of 2000 rpm, corresponding to roughly a rotor tip speed of V_t = 20 m/s. Then, the feed pump frequency (*i.e.* feed flow rate Q_f) and accept and reject valves were adjusted to match the desired average slot velocity V_s and reject ratio of R_v = 0.2. Here, V_s is the average velocity in the apertures and R_v is the ratio of reject flow to feed flow. Several slot velocities were tested in the range of $V_s \in$ [0.5 to 3.5 m/s] for each trial. The rotor speed was progressively decreased in a step-wise manner until an abrupt change in the pressure differential ΔP (difference between the feed and accept pressures) and accept flow was detected, indicating screen plugging (Estevez-Reyes 1995). A 60 second interval between changes in V_t was allowed for the measurements to reach steady conditions.

After plugging occurred and the trial was finished, the screen apertures were cleared by increasing the rotor speed back to 2000 rpm or until the pressure differential was restored to their initial value. However, in some cases, it was necessary to stop the trial and take apart the screen cylinder to manually remove the plugs. Once normal screen operation was restored, the above procedure was repeated for a different configuration of slot velocity, screen cylinder or pulp suspension.

RESULTS AND DISCUSSION

Screen Operational Window

This work included a series of screening trials (Table 1) with different pulp furnishes and screen cylinders to study the effect of ℓ/w and other operating parameters on the screen operating window and plugging. The pressure differential (feed minus accept pressures) was monitored to detect plugging. Figure 2 displays sample plots of the pressure differential ΔP and rotor speed N signals as function of time for water (ℓ/w = 0) and kraft pulp (ℓ/w = 16).

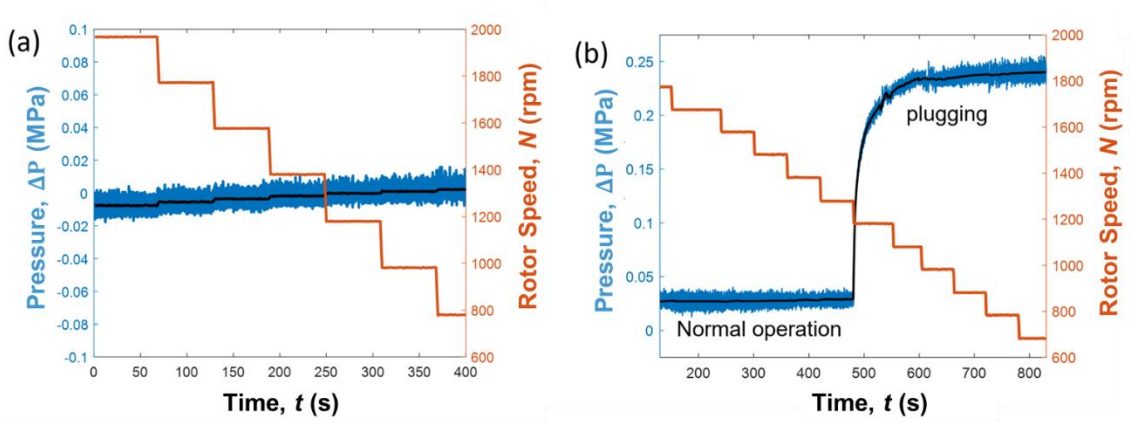

Fig. 2. Sample signals of the pressure differential ΔP (blue) and rotor speed N (orange) as function of time for (a) water and (b) NBSK pulp. The black lines represent the moving average of the pressure signal.

For the water data, the mean and fluctuation of the pressure signal remained relatively constant as the rotor speed was decreased (Fig. 2a). From the pressure signal of the NBSK pulp (Fig. 2b), the plugging event was identified as the point where the pressure increases, defining the transition from the operational to the plugging regime.

The stable screening operation for pulp is the region where the average pressure signal remains relatively constant following a similar behavior to the water pressure signal. In this regime, it is expected that the rotor is fluidizing the suspension as it approaches the apertures. Fibres are being deposited in the apertures, but they are quickly back-flushed by the rotor. The screen stops operating normally at a threshold rotor speed. Beyond the threshold, permanent plugging occurs at the point where the pressure signal sharply rises in the space of a few seconds and, without intervention, it becomes irreversible. In this state, most apertures become blocked. To compensate, the pressure rises to push pulp through the remaining open apertures. The rate at which pressure rises depends on the pulp type and slot velocity. In general, the curve is sharper when the screen is operated at higher slot velocities due to the faster fibre deposition. Eventually, the pressure differential signal starts to reach a plateau, which likely results from the compaction of the plugs. The plugs become strong enough that the rotor speed cannot restore the normal screening operation. At this point, the flow through the apertures becomes just a small fraction of its original value and most of the pulp flows out the reject line. Sample images of compact plugs stuck in the screen apertures after the trial are shown in Fig. 3 from the point of view of both the feed and accept sides of the screen.

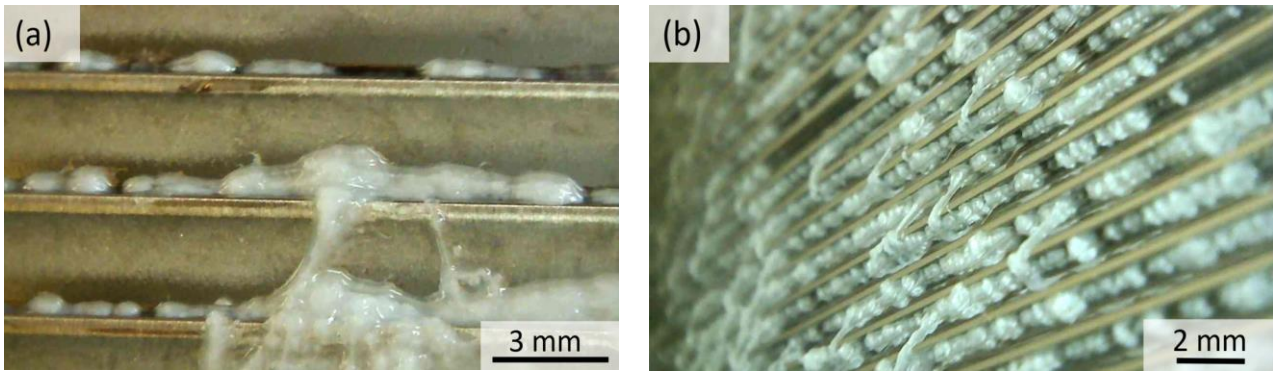

Fig. 3. Sample images of plugs in the apertures from (a) small region from the feed side of the screen and (b) from the accept side of the screen

Using the pressure data as a guide (see Fig. 2), the limits of screening operation are identified as the last operating point prior to plugging. These points are plotted in V_s vs. V_t contours, as shown in Fig. 4a- c for different pulp suspensions. The symbols in the contours denote the points where the screen plugs irreversibly. Consistent with the literature (Delfel 2009; Salem 2013), the curves were remarkably linear for all pulp furnishes and screen geometries. The operational window or the range of allowable rotor speeds depended on the slot velocity V_s and the ratio of the fibre to slot width ℓ/w. Notably, below ℓ/w = 1.5, plugging did not occur even at low rotor speeds (see Fig. 4c) under the experimental conditions presented here.

Effect of Size Ratio on Plugging

The fibre length to slot width ratio ℓ/w plays a role in the passage of fibres (Ashok 1991; Olson 1996), as well as in the plugging of fibres flowing through constrictions (Redlinger-Pohn *et al*. 2021; Villalba *et al*. 2023). In the context of the screening limits, ℓ/w also seems to play a key role. Figure 4 shows that the larger the value of ℓ/w, the narrower was the operating range of the screen. The reduction in the operating window with increasing ℓ/w likely comes from the increased flocculation in the apertures occurring

due to longer fibres or the increased confinement. Indeed, it has been shown that the degree of fibre flocculation is a function of fibre length (Kerekes and Schell 1992; Kerekes 2006), and that ℓ/w affects the degree at which flocs block apertures (Villalba *et al*. 2023).

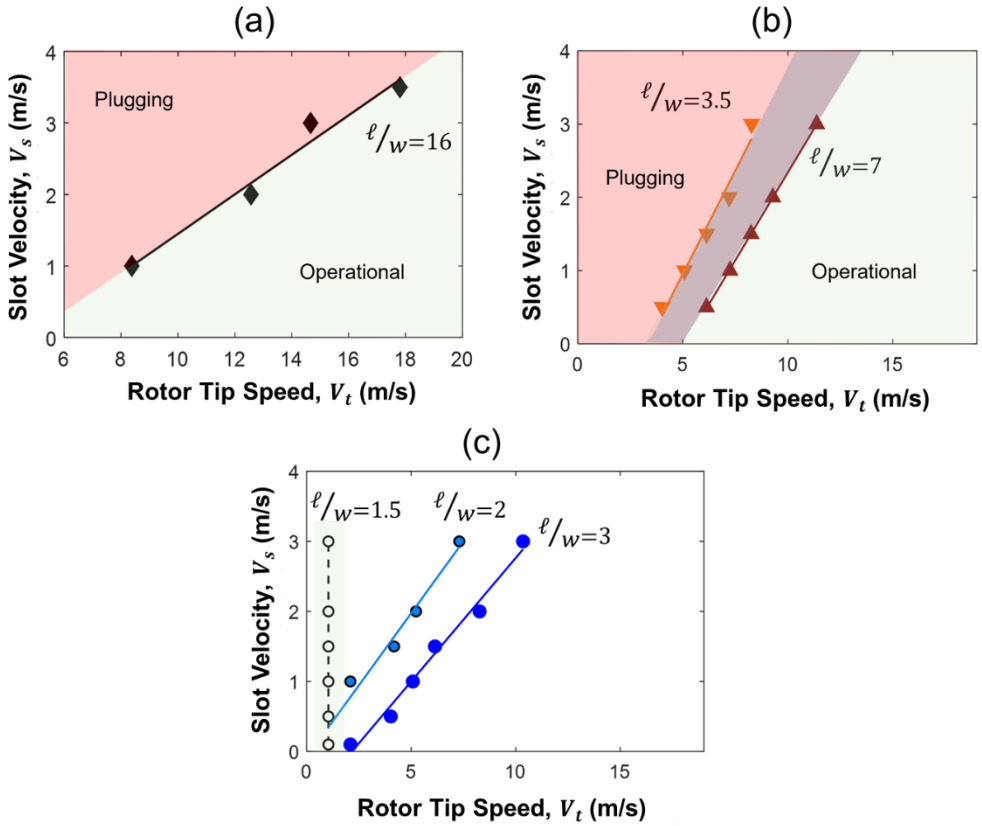

Fig. 4. Limits of screening operation given by $V_s - V_t$ curves for (a) NBSK pulp, (b) eucalyptus pulp and (c) short-fibre mix pulp. The operating range is defined as any point before the pressure differential increases sharply, as shown in Fig. 2. The symbols and line denote the points where the screen plugged permanently. All pulps have 1.0% consistency. The lines show the linear fit of the data with R-squared greater than 0.95.

This became evident when the *x*-intercepts of the extrapolated curves were computed from Fig. 4; notably, they varied with ℓ/w. This intercept is the case where V_s = 0 m/s, which represents the hypothetical minimum rotor speed V_{tm} to keep a floc in place according to the force balance model postulated by Martinez *et al.* (1999). When plotting the intercepts V_{tm} as function of ℓ/w in Fig. 5, V_{tm} is a function of ℓ/w, and it follows a sigmoidal form. From this curve, it becomes more evident that plugging does not occur in the limit $\ell/w \leq 1.5$. This criterion could be related to the average size of pulp flocs which is of the order of 2 fibre lengths (Kerekes 2006). On the other end of the curve, the minimum rotor speed reached a plateau at $V_{tm} \approx 5$ m/s in the limit $\ell/w > 5$, suggesting a different plugging mechanism for long fibres. In this limit, large fibre mats (large, connected flocs) form (Yu and Defoe 1994), which may cause plugging of the screen cylinder regardless of the size of the apertures. Note that the minimum rotor speed is also a function of pulp consistency and rotor type. As these parameters were kept constant here, further work is needed to evaluate their effects on the limits of screening operation.

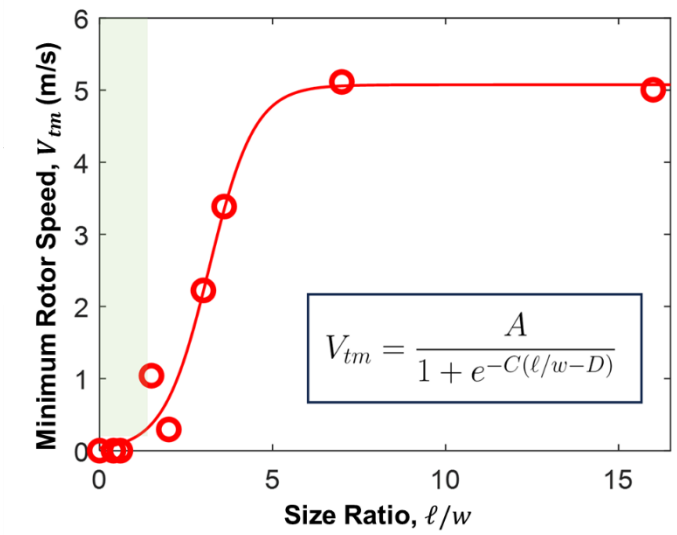

Fig. 5. Minimum rotor speed $\boldsymbol{V_{tm}}$ denoted by the x-intercept of Fig. 4 as function of $\boldsymbol{\ell/w}$ for different *c* = 1.0% pulp suspensions and water. The green region represents the regime where the screen does not plug. The line shows a sigmoidal function as the fit with R-squared of 0.98 and fitting parameters A = 5, C = 1.5, and D = 3.2.

Application of the Prediction Tool for Plugging

Thus far, plugging occurs at a critical rotor speed, which depends on the slot velocity, pulp parameters (ℓ, c), and screen geometries (w). In part one of this work, it was observed that, even before this critical rotor speed was reached, the plugging events displayed an intermittent behavior that intensified near screen failure. Hence, it was hypothesized that the intermittency is a precursory event indicating the onset of screen plugging. In this paper, the fluctuation of the pressure data was scrutinized as a proxy of intermittency (Fig. 2) to get insights into the global behavior of the screen with the purpose of assessing the predictive tool for plugging from part one. To reiterate, the fluctuation component of the signal was isolated by subtracting the moving average from the raw signal data (Eq. 2 of part one). To characterize the intermittency, the distribution of the fluctuation peaks Z_p was plotted in the form of probability density functions $\Psi(Z_p)$ in the same way as in part one.

The typical probability distribution for the water signal is shown in Fig. 6. The distribution of the fluctuation peaks for water seemed to follow the shape of a Gaussian distribution, shown as a black dashed line in the figure. Similarly, the shape of the distribution of the fluctuation peaks Z_p for pulp in the operational state also closely followed a Gaussian distribution, as shown in Fig. 6b. Loosely speaking, the screen seemed to operate in a similar way for water as for pulp, particularly at high rotor speeds. This implies that the pulp is fully fluidized in the operational regime (Bennington and Kerekes 1996). However, as the rotor speed was decreased, the distribution shifted away from the Gaussian form with the fluctuations increasing prior and during plugging. Figure 6c shows a change in the distribution, which now has higher arch and asymmetric tails. Similarly to the open area data from part one of this work (in press), a shift in the distribution of the pressure fluctuations effectively signals the transition from the operational to the plugged state.

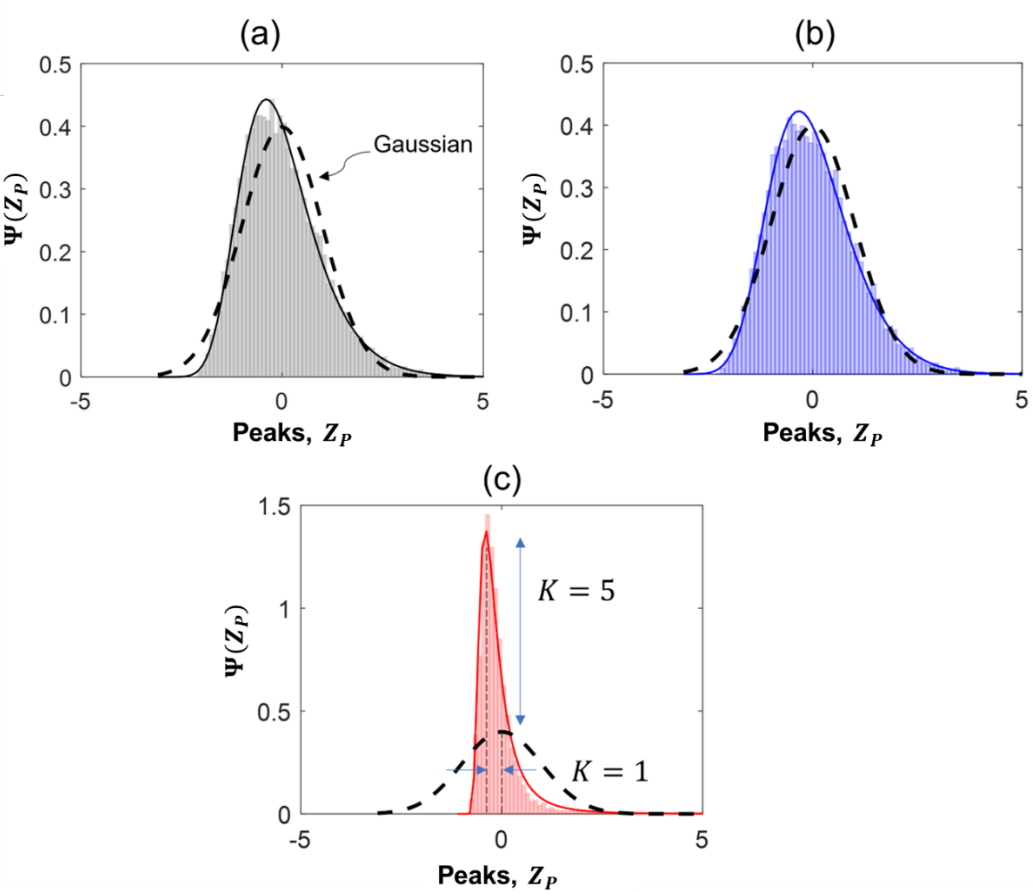

Fig. 6. Sample probability density function $\Psi(Z_p)$ of the normalized fluctuation peaks Z_p of the pressure differential for (a) water (b) *c* = 1.0% NBSK pulp in the operating regime and (c) *c* = 1.0% NBSK pulp during plugging. Data comes from the pressure signal from Fig. 2. The dashed line represents a Gaussian distribution. Values of kurtosis K are displayed in panel (c) for comparison.

Following from part one (Villalba *et al.* 2024), the change in the distribution was quantified using the kurtosis. The distributions of the water and pulp data in the operational regime (see Fig. 6) exhibited kurtosis values close to one with K = 1.16 for water and K = 1.12 for pulp. On the other hand, the kurtosis of the distribution of Z_p during plugging increased up to K = 5, as can be seen in Fig. 6c. Potentially, the shift of the pressure data to the end tails of the distribution indicates higher intermittency, as was the case for the open area data in part one of this work.

The evolution of the kurtosis values as the screen deviated from the operational to the plugging state is shown in Fig. 7, which shows the kurtosis of the pressure fluctuation peaks as function of rotor speed for different pulp suspensions. Kurtosis values for the water data are also plotted in the figures for reference. During normal operation, the kurtosis of the pulp data closely followed that of water with values close to one, which is characteristic of a Gaussian distribution. Evidently, the kurtosis started to increase slightly even before the plugging state was nominally detected as the sharp pressure rise. This finding was robust for different pulp suspensions (see Fig. 7a-c) and screen operating conditions and validates the utility of this tool as a soft-sensor to detect plugging. Further work is needed to characterize the intermittent behavior near the limits of operation for different pulp consistencies, rotor types, and with a vertical screen configuration. In

particular, direct measurements of pressure in the screen apertures would further reinforce the results presented in this study and allow for effective tuning of the rotor pressure pulses to the intermittency of plugging events.

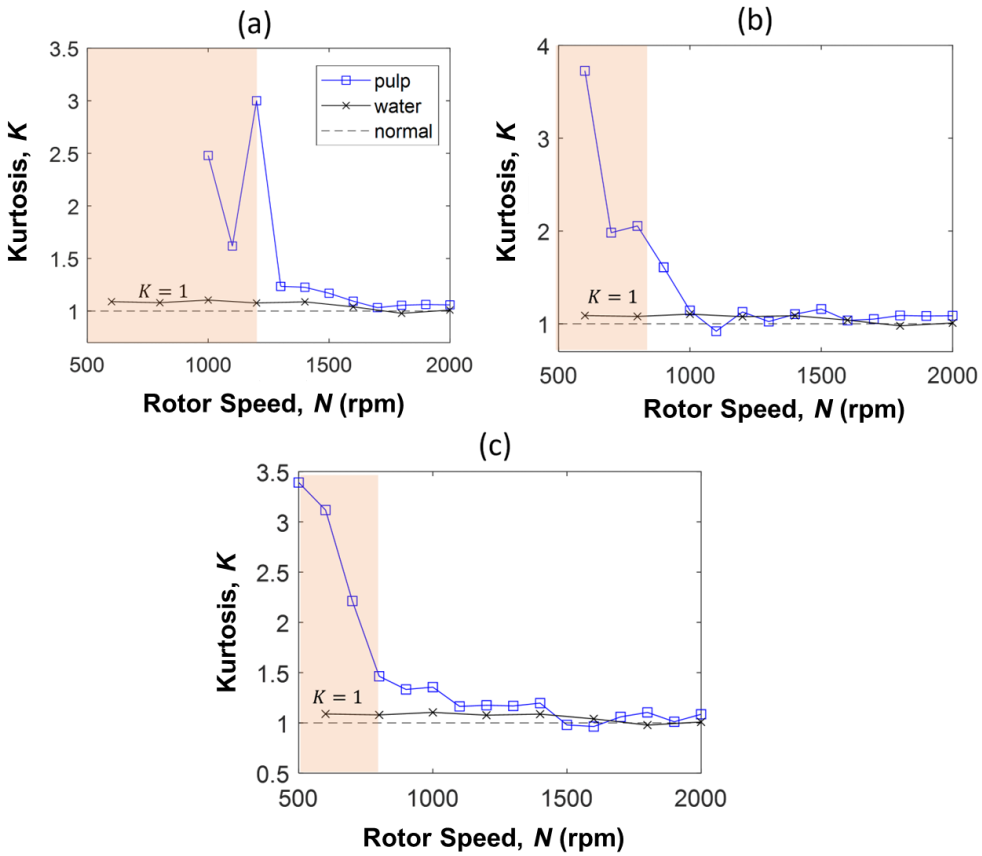

Fig. 7. Kurtosis as function of rotor speed for (a) NBSK pulp (ℓ/w = 16), (b) Eucalyptus pulp (ℓ/w = 3.5) and (c) Hardwood mix pulp (ℓ/w = 3). In all cases, V_s = 2 m/s. The orange region denotes the permanent plugging regime nominally determined by the rise of pressure.

Overall, this two-part investigation has shed light on the limits of screening operation. Notably, an intermittency in the plugging events is unraveled, and through its characterization, the limits of operation are predicted for the experimental conditions tested. These findings are valuable for screen manufacturers to better understand the design factors limiting the screening operation.

CONCLUSIONS

1. The limits of screening operation were outlined with a $V_s - V_t$ contour plot, and a linear relationship at the point of screen plugging was confirmed. This is in line with previous screening studies.
2. The contour V_s = 0 m/s can be interpreted as the force imparted by the rotor to remove a plug. The minimum rotor speed V_{tm} on this contour was estimated, and it varied in a sigmoidal fashion with the ratio of fibre length to slot width, with $\ell > 5w$ then V_{tm} = 5 m/s. Notably, with $\ell/w \leq 1.5$ the screen did not plug under the conditions tested.

3. Following from the methodology developed in part one, the fluctuation of the pressure signal from the trials was scrutinized, and the probability distribution of the fluctuation peaks $\Psi(Z_p)$ was used as proxy of the intermittent behaviour of plugging. For water and under normal operating conditions, the distributions $\Psi(Z_p)$ adopt a Gaussian form. The distribution $\Psi(Z_p)$ deviates from Gaussian and starts to skew as the definite plugging point is reached.
4. The change in the distribution with the kurtosis *K* was characterized, and it was used as a metric to detect the onset of plugging with the pressure data. The kurtosis increases as the screen approaches the permanent plugged state further validating this tool as a soft-sensor to detect plugging in pilot-scale screening operations.

ACKNOWLEDGMENTS

The financial support through the NSERC Collaborative Research program, Canada, in conjunction with Aikawa Fiber Technologies Inc., is gratefully acknowledged.

REFERENCES CITED

Ashok, K. (1991). *Passage of Fibres through Screen Apertur*es, Ph.D. Dissertation, University of British Columbia, Canada.

Bennington, C. P., and Kerekes, R. J. (1996). "Power requirements for pulp suspension fluidization," *Tappi Journal* 79, 253-258.

Delfel, S. (2009). *A Numerical and Experimental Investigation into Pressure Screen Foil Rotor Hydrodynamics*, Ph.D. Dissertation, University of British Columbia, Canada.

Estevez-Reyes, L. W. (1995). *Fault Detection on Pulp Pressure Screens*, Ph.D. Dissertation, University of British Columbia, Canada.

Kerekes, R., and Schell, C. (1992). "Regimes by a crowding factor," *J. Pulp Pap. Sci.* 18, J32-38.

Kerekes, R. J. (2006). "Rheology of suspensions: Rheology of fibre suspensions in papermaking: An overview of recent research," *Nordic Pulp & Paper Research Journal* 21, 598-612.

Martinez, D. M., Gooding, R. W., and Roberts, N. (1999). "A force balance model of pulp screen capacity," *Tappi Journal* 82, 181-187.

Olson, J. A. (1996). *The Effect of Fibre Length on Passage through Narrow Apertures*, Ph.D. Dissertation, University of British Columbia.

Redlinger-Pohn, J. D., Liverts, M., and Lundell, F. (2021). "Parameter regimes and rates of fibre collection on screens of various design," *Separation and Purification Technology* 259(15), article 118053. DOI: 10.1016/j.seppur.2020.118053

Salem, H. J. (2013). *Modeling the Maximum Capacity of a Pulp Pressure Screen*, Ph.D. Dissertation, University of British Columbia, Canada.

Villalba, M. E., Daneshi, M., and Martinez, D. M. (2023). "Characterizing jamming of dilute and semi-dilute fiber suspensions in a sudden contraction and a t-junction," *Physics of Fluids* 35(12), article no. 123339. DOI: 10.1063/5.0178933

Villalba, M. E., Olson, J. A., and Martinez, D. M. (2024). "Understanding the limits of a screening operation. Part 1: Characterization of screen plugging," *BioResources* 19(2), 2404-2416. DOI: 10.15376/biores.19.2.2404-2416

Yu, C., and Defoe, R. (1994). "Fundamental study of screening hydraulics. Part 1: Flow patterns at the feed- side surface of screen baskets; mechanism of fiber-mat formation and remixing," *Tappi Journal* 77, 219-226.

Article submitted: January 26, 2024; Peer review completed: February 17, 2024; Revised version received: March 19, 2024; Accepted: March 20, 2024; Published: March 25, 2024.
DOI: 10.15376/biores.19.2.2990-3000